Effect of diatomic islands on step morphological stability of a terrace edge in molecular beam epitaxy

Senpuu Lin[a,*], Chi-Chuan Hwang[b], Hsin-Sen Chu[c]

[a]*Department of Mechanical Engineering, National Lien-Ho College of Technology and Commerce, P.O. Box 12-2, Miao-Li, Taiwan 36012, People's Republic of China*
[b]*Department of Mechanical Engineering, Chung Yuan University, Chung Li, Taiwan 32023, People's Republic of China*
[c]*Department of Mechanical Engineering, National Chiao Tung University, Hsinchu, Taiwan 30050, People's Republic of China*

Abstract

The effect of two-dimensional diatomic-island nucleation on the linear stability of the step morphology during molecular beam epitaxy is investigated numerically via shooting methods. It is found that the effect of diatomic islands on the step morphological stability is significant. The greater the effects of diatomic islands, the more stable the step morphology. Increasing capture efficiency can decrease the critical surface capillary length and shift the critical wave number toward short-wavelength regimes. The unstable region is shrunk with increasing capture efficiency. Further, increasing flux coverage and/or surface coverage can decrease the critical surface capillary length and shift the critical wave number toward short-wavelength regimes. © 1999 Elsevier Science S.A. All rights reserved.

1. Introduction

Many semiconductors are manufactured by molecular beam epitaxy (MBE). The ability to grow crystals with essentially monolayer composition in atom scales is considerably important in the fabrication of devices [1]. Ideally, it results in terraces separated by monoatomic straight steps with atoms diffusing on the terraces and the morphology of the terrace edges is not changing its shape by the advancement of a uniform stable step train [2].

The problem of such a step flow was discussed in a seminal paper by Burton, Cabrera and Frank [3] (BCF). However, as experimental studies have demonstrated, the terrace edges of the straight step display quite often a wavy nature [4]. It was shown by Bales and Zangwill [5] in 1990 from a linear stability analysis, taking into account Schwobebel effect [6] and stationary condition, that a terrace edge can undergo a morphological instability if a grow rate exceeds a critical value. The stabilizing effect is due to the line tension of the step that prevents short-wavelength deformations. The instability mechanism is much like the so-called Mullins-Sekerka instability [8]. As the straight step becomes unstable, non-linear effects evolve quickly

in the growth dynamics. In 1993, Bena, Misbah, and Valance [9] performed a weakly non-linear analysis of the step flow near the threshold of the instability for the 'one-sided' model (i.e. complete blocking from the upper terrace). The result is a Kuramoto–Sivashinsky-type equation [10,11], which exhibits spatiotemporal chaos. More kinetic instabilities of the step morphology under the lateral and/or the longitudinal fluctuation with/without the presence of the external direct electric field have been investigated [12–28]. Although they have extended the ideal BCF theory to MBE none has explicitly incorporated and determined the effects of two-dimensional cluster nucleation on the terrace.

In the ideal BCF theory, linear-diffusion equation is used to determine the step velocity and distribution of adsorbed atoms (or adatoms, for short) on the terrace. To explain the measurements of an oscillating RHEED (reflection high-energy electron-diffraction) intensity during MBE growth, Myers-Beaghton and Vvedensky [29–31] postulated that a model for MBE must include both the migration of adatoms on the substrate and the interaction among these adatoms in the form of incipient cluster formation. They then introduced a non-linear diffusion equation, an extension of the linear BCF equation, by including a quadratic interaction as a first-order approximation to incipient cluster formation.

In this paper we study the effect of two-dimensional

---

* Corresponding author. Fax: +886-3-736-4145.
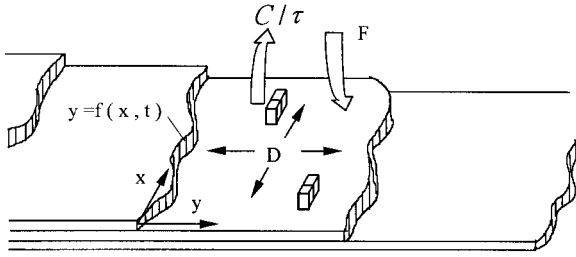*E-mail address:* spuulin@mail.lctc.edu.tw (S. Lin)

Fig. 1. Schematic view of a vicinal surface during step flow with two-dimensional diatomic-island nucleation on the terrace.

nucleation, due to the lateral adatom interactions in the form of diatomic island formation on the terrace, on linear stability in the step morphology of a terrace edge during MBE. The non-linear diffusion equation and the one-sided model of an isolated step are adopted to describing epitaxial growth in MBE. The linear stability analysis is performed numerically via shooting methods.

2. Formulation

Consider the mathematical formation of the original BCF model [3], for a close-packed face of a crystal, growing from a supersaturated mother medium. We concentrate on the epitaxial growth mechanism characterized by the diffusion-controlled propagation of a single atomic step, and take account of the effect of incipient two-dimensional diatomic-island nucleation, under the assumption of a moderate supersaturation during MBE. A complete model for MBE must include both the migration of adatoms on the terrace and the lateral interactions among these adatoms for incipient cluster formation [29–31]. The schematic view is shown in Fig. 1. A flux of atoms impinges upon the substrate from a gas atmosphere with a frequency F per unit area and time. Adatoms migrate on the facet with a diffusion constant D, but after a lifetime τ they are desorbed. During the surface diffusion, adatoms collide to form two-dimensional diatomic islands, which then form capture sites that compete with the step edge as sinks for the migrating adatoms. Then, a single atomic step on the crystal surface is advancing slowly in the y direction at the expense of the gas atmosphere. There is usually an asymmetry in the attachment kinetics of adatoms at a step from the lower and from the upper terraces, called the Ehrlich–Schwoebel effect [6,7]. It is widely admitted that adatoms can be incorporated to the step only from the terrace that is ahead (the lower one in Fig. 1) of the advancing step. This corresponds to the so-called one-sided model [5,9]. It is the extreme case. We assume that the growth is governed only by adatoms on that terrace, and can proceed by two-dimensional diatomic-island nucleation and step flow simultaneously. For this simply case of an isolated step in one-sided model, it is also assumed that the steps, advancing very slowly without any interactions between the step and its neighbors, are very far

apart. According to the works of Myers-Beaghton and Vvedensky [29–31], the concentration of single adatoms on the terrace $C(x,y,t)$ satisfies the non-linear continuity equation

$$\frac{\partial C}{\partial t} = D\left(\frac{\partial^2 C}{\partial x^2} + \frac{\partial^2 C}{\partial y^2}\right) - \frac{C}{\tau} + F - R(C(x,y,t)) \qquad (1)$$

where the function $R(C(x,y,t))$, which incorporates the removal of two adatoms per diatomic-island cluster formed on the terrace, is given by

$$R(C(x,y,t)) = 2\sigma D C^2 + 2Fm\frac{C}{C_i} \qquad (2)$$

To be consistent, it is assumed that once an island is formed, the emission of adatoms from cluster and step edge is forbidden and the island is immobile. The first term on the right-hand side of Eq. (2) represents the rate at which single migrating adatoms collide to form diatomic islands and is proportional to D and to σ, a capture efficiency of order one [29,32]. The second term accounts for the direct collision of incoming atoms with adsorbed atoms and is proportional to the total fraction of incoming adatoms that arrive at island-forming sites, C/C_i, where C_i is the concentration of lattice sites. The factor m is the number of sites around a single adsorbed atom that will form a diatomic island when filled. For a square lattice, $m = 5$, corresponding to the four nearest neighbors and the site of the adsorbed atom. The factors of two accounts for the fact that two adatoms are lost for every diatomic island formed.

The problem is completely specified by choice of the boundary conditions for Eq. (1) and the requirement of mass conservation at the step. Let $y = f(x,t)$ denote the trajectory of the step edge in the plane of the surface. The amount by which each point on the step advances in the normal direction is determined by the concentration gradient in the same direction. Precisely the normal velocity v_n is proportional to the normal derivative of concentration

$$V_n \Omega^{-1} = D\frac{\partial C}{\partial n} \qquad (3)$$

where Ω is the atomic area of the solid, we can write $\Omega = 1/C_i$. The step normal $\hat{n} = (-\partial f/\partial x, 1)/\sqrt{1 + (\partial f/\partial x)^2}$ is a unit out of the solid perpendicular to the step riser. Since the basic state will be a straight step advancing at a constant velocity v in the y direction. The normal velocity takes the form

$$V_n = \frac{V + \partial f/\partial t}{\sqrt{1 + (\partial f/\partial x)^2}} \qquad (4)$$

Then, the Eq. (3) will become

$$\left(V + \frac{\partial f}{\partial t}\right)C_i = D\left(\frac{\partial C}{\partial y} - \frac{\partial f}{\partial x}\frac{\partial f}{\partial x}\right) \qquad \text{at } y = f(x,t) \quad (5)$$

Another boundary condition relates the concentration of adatoms at the step edge, which is modified to account for

local step curvature using the Gibbs–Thompson equation [5,9,14,24]

$$C \equiv C_{\text{step}} = C_{\text{eq}} \left[1 - \frac{\gamma \Omega}{k_{\text{B}} T} \frac{\partial^2 f / \partial x^2}{\left[1 + \left(\partial f / \partial x \right)^2 \right]^{3/2}} \right]$$

at $y = f(x, t)$ (6)

where C_{eq} is the equilibrium concentration of adatoms for a straight step edge, γ is the isotropic line tension of the step, k_{B} is the Boltzmann constant, and T is the fixed substrate temperature. We should mention that crystalline anisotropy (which can enter the diffusion coefficient and the line tension) is not accounted for in the present work.

Finally, the concentration of adatoms far away from the step ($y \rightarrow \infty$, i.e. for a distance larger than the surface diffusion length to be introduced below) is maintained above the equilibrium value C_{eq} through supersaturation for typical MBE condition. And, it should reach a constant value $C_\infty > C_{\text{eq}}$, which simply expresses the equilibrium among deposition, evaporation and diatomic islands on the terrace. At equilibrium, there is no time dependence and there are no concentration gradients, so that C_∞ can be reduced from the non-linear continuity Eq. (1), given by

$$C_\infty = \frac{1}{4\sigma D \tau C_i} \left\{ \left[(C_i + 2m\tau F)^2 + 8\sigma D C_i^2 \tau^2 F \right]^{1/2} - C_i - 2m\tau F \right\}$$

(7)

The set of Eqs. (1)–(7) completely describes the step growth which occurs both through the adsorption of single atoms onto the terrace and their subsequent diffusion into the terrace edge as well as two-dimensional diatomic-island nucleation through adatom collisions. Since the concentration of lattice sites C_i also can be written to $1/\Omega$, we introduce a characteristic distance $x_{\text{s}} \equiv \sqrt{(D\tau)}$ (which we usually call the surface diffusion length) and the equilibrium flux $F_{\text{eq}} \equiv C_{\text{eq}}/\tau$, and employ the following non-dimensionalization

$$x = x_s \bar{x}, y = x_s \bar{y}, f = x_s \bar{f}, t = \tau \bar{t}, V = x_s \bar{V}/\tau, C = C_{\text{eq}} \bar{C},$$

$$C_\infty = C_{\text{eq}} \bar{C}_\infty$$ (8)

then the above non-linear continuity Eq. (1) will become (with overbars omitted, from now on, only dimensionless variables)

$$\frac{\partial C}{\partial t} = \frac{\partial^2 C}{\partial x^2} + \frac{\partial^2 C}{\partial y^2} - 2\sigma \frac{\alpha \beta}{1 + \lambda} C^2$$

$$-(1 + 2m\alpha)C + 1 + \lambda$$

in $y > f(x, t)$ (9)

Eqs. (5) and (6), the boundary conditions at the step, are to be, respectively,

$$V + \frac{\partial f}{\partial t} = \frac{\alpha}{1 + \lambda} \left(\frac{\partial C}{\partial y} - \frac{\partial f}{\partial x} \frac{\partial C}{\partial x} \right) \text{ at } y = f(x, t)$$ (10)

$$C = 1 - \xi \lambda \frac{\partial^2 f / \partial x^2}{\left[1 + \left(\partial f / \partial x \right)^2 \right]^{3/2}} \qquad \text{at } y = f(x, t)$$ (11)

and Eq. (7), the adatom concentration far away from the step, can be rewritten as

$$C \equiv C_\infty = \frac{1 + \lambda}{4\sigma \alpha \beta} \left\{ \left[(1 + 2m\alpha)^2 + 8\sigma \alpha \beta \right]^{1/2} - 1 - 2m\alpha \right\}$$

as $y \rightarrow \infty$ (12)

where $\lambda \equiv (F - F_{\text{eq}})/F_{\text{eq}}$ is the dimensionless relative supersaturation ratio, providing the driving force, $\xi \equiv \gamma \Omega/(k_{\text{B}} T x_{\text{s}} \lambda)$ is the dimensionless surface capillary length, $\alpha \equiv \Omega \tau F$ is the flux coverage, and $\beta \equiv x_{\text{s}}^2/\Omega$ is the surface coverage. The non-dimensional λ, ξ, α, β, σ and m govern the behavior of the system. It is noted that surface capillary length ξ is the ratio of the step line tension to the thermal excitation energy through supersaturation. The flux coverage α is a small number, whereas the surface coverage β is a large number for typical MBE condition, according to the works of Myers-Beaghton and Vvedensky [29–31], for $1 > \alpha > 1/\beta$, adatoms interact to form diatomic islands on their diffusion path to the step - that is, two-dimensional nucleation competes with step flow. While, in the case of neglecting the effect of two-dimensional diatomic-islands nucleation, as the capture efficiency $\sigma = 0$ and the nucleation factor $m = 0$, the linear BCF equations is recovered. The step is assumed to advance slowly and the adatoms concentration relaxes so fast that the stationary condition $\partial C/\partial t = 0$ is realized.

3. Basic state solution

We first seek the basic state solution of the non-dimensional Eqs. (9)–(12), i.e. the time derivative does not appear in the equations and it is a function of y only. Let $C_0(y)$ denote the corresponding concentration profile of the basic state (a straight step, which we take at $y = 0$). Consequently, the non-dimensional non-linear continuity Eq. (9) can be reduced to

$$\frac{d^2 C_0}{dy^2} - 2\sigma \frac{\alpha \beta}{1 + \lambda} C_0^2 - (1 + 2m\alpha)C_0 + 1 + \lambda = 0$$

for $y > 0$ (13)

Eqs. (10) and (11), the non-dimensional boundary conditions at the step for the conservation of materials, will become, respectively,
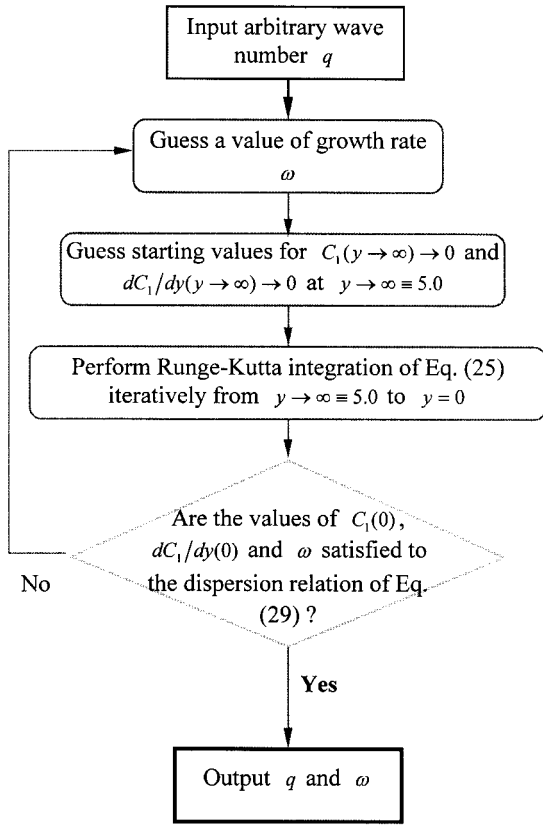
Fig. 2. Flow chart of numerical analysis for dispersion relation via shooting method.

$$V = \frac{\alpha}{1+\lambda}\frac{dC_0}{dy} \qquad \text{at } y = 0 \tag{14}$$

$$C_0 = 1 \qquad \text{at } y = 0 \tag{15}$$

Eq. (12), the equilibrium condition that is far away from the step, is written to be

$$C_0 = C_\infty \qquad \text{as } y \to \infty \tag{16}$$

Obviously, since it is very difficult to find the solution of Eqs. (13)–(16) by the analytical method, we proceed via shooting methods numerically from $y \to \infty \equiv 5.0$ to $y = 0$ by assuming a value for $dC_0/dy(y \to \infty) \to 0$ with the starting value of $C_0(y \to \infty) = C_\infty$, and iteratively performing the Runge–Kutta integration to $y = 0$ until the assumed value for $dC_0/dy(y \to \infty) \to 0$ is one that yields $C_0(0) = 1$. Successive improved guesses of $dC_0/dy(y \to \infty) \to 0$ are found using the half-interval method [33]; the solution converges rapidly. Once the solution of basic state concentration $C_0(y)$ is obtained, the dimensionless advancing velocity v of the straight step can be calculated from Eq. (14).

4. Linear stability analysis

The linear stability analysis is the first step towards the understanding of the mechanisms by which a new structure can be formed. The main outcome of a linear stability analysis is the determination of the critical condition of the onset of the instability, and the range of wave numbers of those perturbations that are likely to grow first.

To study the roughness of the terrace edge in a linear-theory way, following the works of Bena et al. [9], let us consider a straight step with an extra small perturbation by setting

$$C(x, y, t) = C_0(y) + C'(x, y, t) \tag{17}$$

$$f(x, t) = 0 + f'(x, t) \tag{18}$$

where $(C_0(y), 0)$ are the basic state solutions, and $C'(x,y,t)$ and $f'(x,t)$ are small perturbations of the system. Substituting Eqs. (17) and (18) into Eqs. (9)–(12) and linearizing the resultant equations, a set of equations which control the developing of small perturbation is derived as follows

$$\frac{\partial^2 C'}{\partial x^2} + \frac{\partial^2 C'}{\partial y^2} - \frac{\partial C'}{\partial t} - 4\sigma\frac{\alpha\beta}{1+\lambda}C_0 C'$$
$$-(1 + 2m\alpha)C' = 0, \qquad \text{in } y > 0 \tag{19}$$

$$\frac{\partial f'}{\partial t} = \frac{\alpha}{1+\lambda}\left(\frac{\partial C'}{\partial y} + \frac{d^2 C_0}{d^2 y}f'\right) \qquad \text{at } y = 0 \tag{20}$$

$$\frac{dC_0}{dy}f' + C' = -\xi\lambda\frac{\partial^2 f'}{\partial^2 x} \qquad \text{at } y = 0 \tag{21}$$

$$C' = 0, \qquad \text{as } y \to \infty \tag{22}$$

Then express the small perturbation by the normal mode

$$C'(x, y, t) = C_1(y)e^{iqx+\omega t} \tag{23}$$

$$f'(x, t) = f_1 e^{iqx+\omega t} \tag{24}$$

where q is the wave number, ω is the growth rate of the perturbation amplitude, and C_1 and f_1 are small quantities. Again, substituting Eqs. (23) and (24) into Eqs. (19)–(22) and linearizing the resulting equations, we obtain the following characteristic equation systems

$$\frac{d^2 C_1}{dy^2} - \left(\omega + q^2 + 1 + 4\sigma\frac{\alpha\beta}{1+\lambda}C_0 + 2m\alpha\right)C_1 = 0$$
$$\text{for } y > 0 \tag{25}$$

$$\frac{\alpha}{1+\lambda}\frac{dC_1}{dy} = \omega f_1 - \frac{\alpha}{1+\lambda}\frac{d^2 C_0}{dy^2}f_1 \qquad \text{at } y = 0 \tag{26}$$

$$C_1 = \xi\lambda q^2 f_1 - \frac{dC_0}{dy}f_1 \qquad \text{at } y = 0 \tag{27}$$

$$C_1 = 0 \qquad \text{as } y \to \infty \tag{28}$$
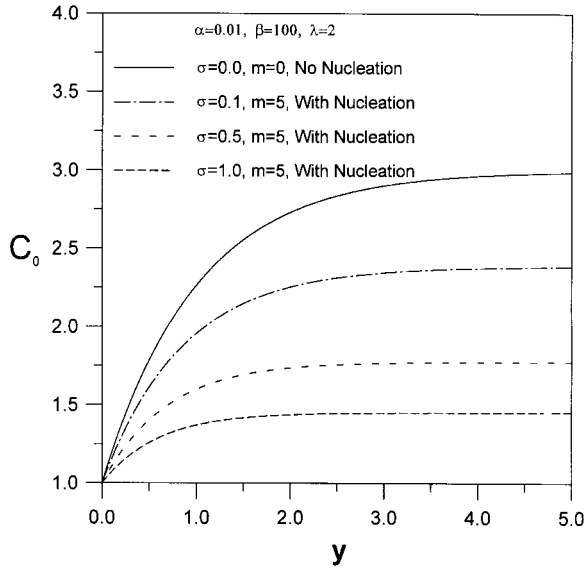
Eliminating from Eq. (26) by Eq. (27) gives the disper-

Fig. 3. Adatom concentration profile $C_0(y)$ along terrace for a basic state (straight step).

sion relation

$$\omega = \frac{\alpha}{1+\lambda}\left\{\frac{d^2C_0}{dy^2}(0) + \frac{\frac{dC_1}{dy}(0)}{C_1(0)}\left[\lambda\xi q^2 - \frac{dC_0}{dy}(0)\right]\right\} \quad (29)$$

After the basic state solution $C_0(y)$ is obtained, the solution of Eqs. (25)–(28) can now be also evaluated by the similar shooting methods in Section 3 via a starting value at $y \to \infty \equiv 5.0$ for $C_1(y \to \infty) \to 0$ and $dC_1/dy(y \to \infty) \to 0$ with arbitrary wave number q and the guess value of growth rate ω. The values of $C_1(0)$ and $dC_1/dy(0)$ as well as ω must be satisfied to the dispersion relation of Eq. (29). It is noted that the Runge–Kutta integration and the half-interval method are also used to solve the problem. The procedure of shooting method is shown schematically in Fig. 2.

The straight step is stable if $\omega < 0$ for all q's. Conversely it is unstable if there exists at least one wave number q for which $\omega > 0$. The critical condition is attained when $\omega = 0$ for a particular value of q, say q_c, while it is negative for all other q's. This occurs when the two conditions

$$\omega(q_c) = 0, \ [\partial\omega/\partial q]_{q=q_c} = 0 \quad (30)$$

are met. These two equations determine the critical condition on the onset of instability and the wave number of the bifurcating mode.

5. Results and discussion

The method to derive the basic-state solutions and their linear stability has been described in Sections 3 and 4. Here we show the results and discuss their characteristics. In case of the dimensionless relative supersaturation ratio $\lambda = 2$, the flux coverage $\alpha = 0.01$, the surface coverage $\beta = 100$, for simplicity, the solutions to $C_0(y)$ are shown in Fig. 3 without two-dimensional diatomic-island nucleation, capture efficiency $\sigma \to 0$ and the nucleation factor $m \to 0$, and with two-dimensional diatomic-island nucleation for the factor $m = 5$ and various capture efficiency σ, respectively. Because adatoms collide to form diatomic islands on the terrace, it results in decreasing the adatom concentration on the terrace. As shown in Fig. 3, the diatomic island effect can depress the basic state of adatom concentration profile along terrace. Furthermore, it is found that increasing σ, i.e. increasing the capture efficiency, makes the effects of diatomic islands stronger, then gradually depresses the profile of basic state of adatom concentration with increasing σ.

According to the results of Bena et al. [9] for the one-sided model of an isolated step without two-dimensional diatomic-island nucleation on the terrace, one can find from Eq. (30) that the bifurcation is characterized by only dimensionless surface capillary length ξ in

$$q_c = 0, \qquad \xi \equiv \frac{\bar{\Gamma}}{x_s\lambda} = \xi_c = \frac{1}{2} \quad (31)$$

where $\bar{\Gamma} = \gamma\Omega/k_BT$ incorporates the isotropic line tension of the step (which has a dimension of a length), $\lambda = (F - F_{eq})/F_{eq}$ is the dimensionless relative supersaturation ratio. As mentioned in the above section, capillary length is the ratio of the step line tension to the thermal excitation energy through supersaturation. It expresses the competition between line tension and the incident flux as agents for mass transport. It is observed that q_c goes to zero abruptly at some critical value ξ_c and thus there is a crossover from morphologically stable step ($\xi > \xi_c$, $\omega < 0$) to morphologically unstable step ($\xi < \xi_c$, $\omega > 0$) [5,9]. This means that the amplification rate $\omega < 0$ for all wave number q's if capillary length $\xi > 0.5$. However, if capillary length $\xi < 0.5$, there exists a band of wave numbers corresponding to unstable modes. This instability is intrinsic; it is driven by diffusion of atoms along the terrace. The step morphological instability can thus take place only if the characteristic surface diffusion length x_s becomes smaller than the typical capillary length determined by the ratio of the line tension to the thermal excitation through supersaturation. The stabilizing effect is due to the line tension of the step, which prevents short-wavelength deformations, and the thermal excitation energy represents the destabilization of diffusion. We can explain that a forward bulge in the terrace edge, in the absence of line tension, steepens the concentration gradient in the terrace ahead of it, which means that the step flows rapidly away from the surface and the bulge grows unstably. Similarly, a depression like that at the concave portion tends to hold the step back. With finite step line tension, however, the curvatures in the terrace edge are such that the concentration is reduced at the convex
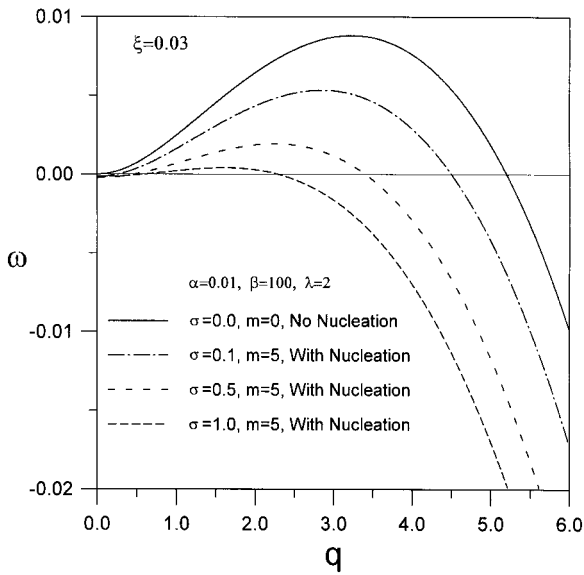
Fig. 4. Growth rate of the perturbation amplititude ω versus wave number q for typical values of the model parameters.

portion and increased at the concave portion. The resulting mass flow from the concave portion to the convex portion tends to restore the flatness of the terrace edge. It is the competition between these two effects that determines the sign of the perturbation amplification rate ω in the dispersion relation of Eq. (29), and thus the overall linear stability of the morphology of a terrace edge in one-sided model for an isolated step during molecular beam eptiaxy.

The growth rate of the perturbation amplitude $\omega(q)$ versus perturbation wave number q for typical values of the model parameters in surface capillary length $\xi = 0.03$ with/without two-dimensional diatomic-island nucleation is
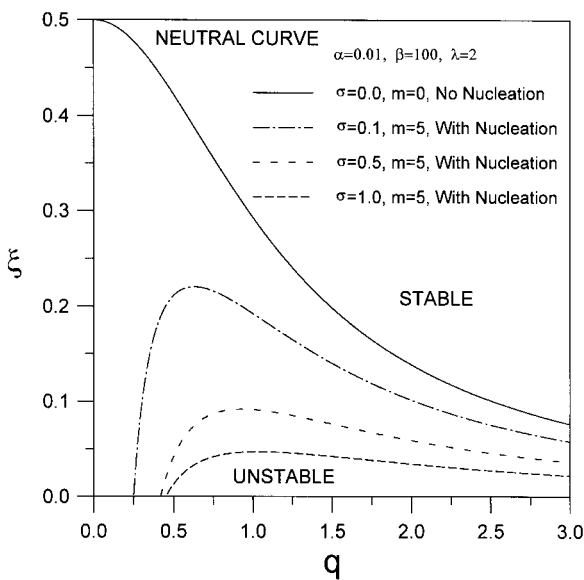

Fig. 5. Neutral stability curves of the step morphology of a terrace edge in ξ–q plane for typical values of the model parameters.
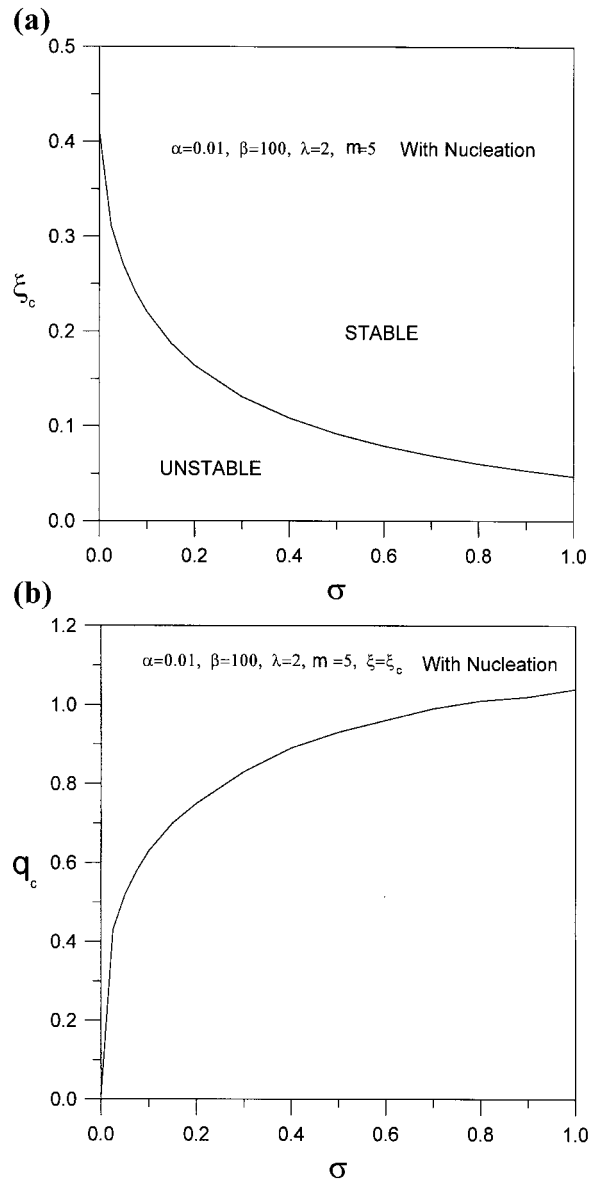

Fig. 6. (a) The variations of critical surface capillary length ξ_c with capture efficiency σ, (b) The variations of critical wave number q_c with capture efficiency σ.

plotted in Fig. 4. A band of wave numbers corresponding to unstable modes is shrunk with increasing capture efficiency σ. Also, the maximum value of the growth rate ω is decreased with increasing σ. The effect of diatomic islands on step morphology is to damp the effects of perturbations from the ideal straight edge. Because the inclusion for adatom clustering on the terrace implies decreasing propensity for thermal promotion of adatoms, it corresponds to an increasing the line tension of the step. For an initial curvature-induced convex portion, the perturbation in the adatom concentration adjacent to a terrace edge is an increase in the local adatom concentration. The propensity to nucleate diatomic islands would result in a decrease in the mobile adatom population. Then, it results in a decrease in the flux
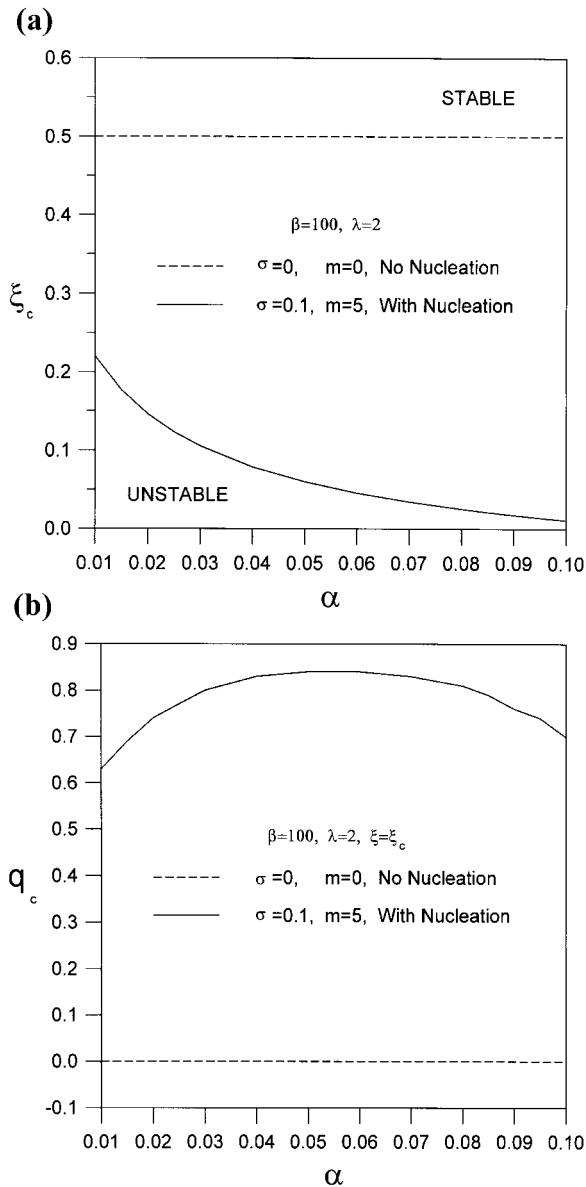
(a)

(b)

Fig. 7. (a) The variations of critical surface capillary length ξ_c with flux coverage α, (b) The variations of critical wave number q_c with flux coverage α.

number of the bifurcating mode, (ξ_c, q_c), with the varying capture efficiency σ in Fig. 6a,b, respectively. It is found that increasing capture efficiency σ can decrease the critical surface capillary length ξ_c shift the critical wave number q_c toward short-wavelength regimes. In comparison with the critical condition of no nucleation, $(\xi_c, q_c) = (0.5, 0.0)$, the effect of two-dimensional diatomic-island nucleation is apparent on the morphological instability of a terrace edge during the moderate supersaturation crystal growth in MBE.

Also, the effects of the flux coverage α on the critical condition of the onset of instability with/without nucleation are demonstrated in Fig. 7a,b. Without nucleation on the
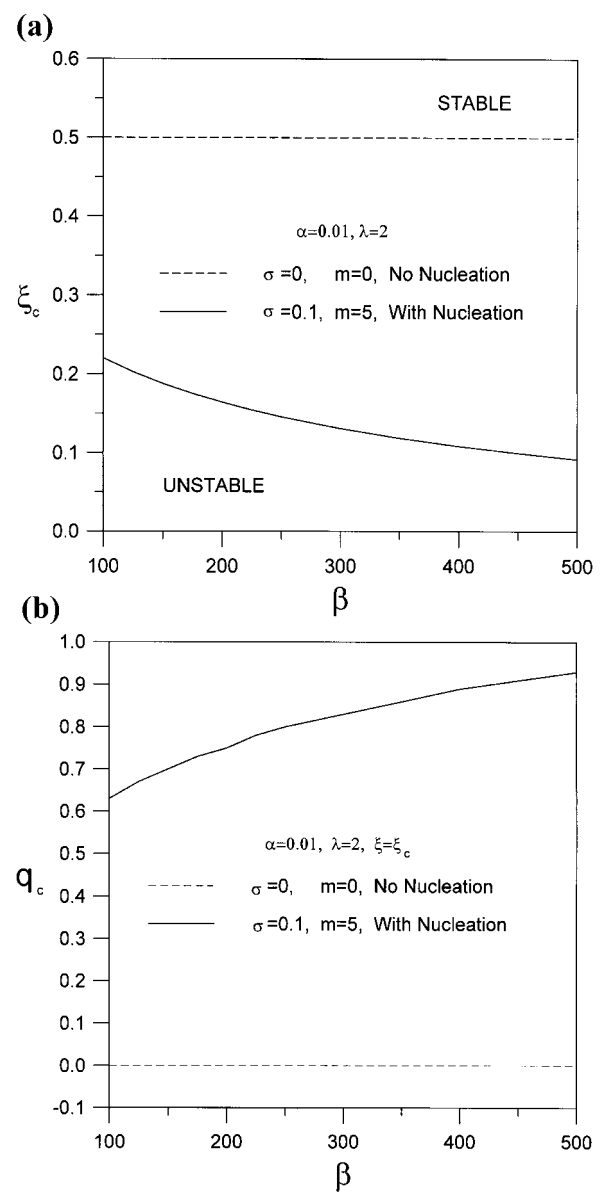
(a)

(b)

Fig. 8. (a) The variations of critical surface capillary length ξ_c with surface coverage β, (b): The variations of critical wave number q_c with surface coverage β.

of mobile adatoms to the terrace edge, which decrease the local velocity away from the step edge that tends to flatten the convexity and diminish the perturbation. The greater is the effect of two-dimensional diatomic-island nucleation, the step morphology is more stable during MBE.

In Fig. 5, the neutral stability curve $\omega(\xi, q) = 0$, there is shown the evidence that the effect of two-dimensional diatomic-island nucleation is stabilizing effect. During moderate supersaturation crystal-growth in MBE, the unstable region is shrunk with increasing capture efficiency σ.

Moreover, we show the critical surface capillary length condition on the onset of instability and the critical wave

terrace, the flux coverage α does not affect the critical condition of the onset of instability during MBE [9]. With nucleation, the critical surface capillary length ξ_c is decreased with increasing flux coverage α and the critical wave number q_c is shifted toward short-wavelength regimes compared the point of $q_c = 0$. That is, the unstable region is shrunk with increasing flux coverage.

Finally, in Fig. 8a,b, the effects of surface coverage β on the critical condition with/without nucleation are investigated. In case of no nucleation, the same as the flux coverage, the critical condition of the onset of instability has nothing to do with the surface coverage. While, with nucleation, increasing surface coverage β can decrease the critical surface capillary length ξ_c and shift the critical wave number q_c toward short-wavelength regimes.

6. Conclusion

The effect of two-dimensional diatomic-island nucleation on the linear stability in the step morphology during molecular beam epitaxy is investigated numerically via shooting method. The non-linear-diffusion governing equation, due to adatom interactions in the form of diatomic island formation, for one-sided model of an isolated step is adopted. It is found that the effect of diatomic islands on the step morphological stability is significant. The greater the effects of diatomic islands, the more stable the step morphology. Increasing capture efficiency σ can decrease the critical surface capillary length ξ_c and shift the critical wave number q_c toward short-wavelength regimes. The unstable region is shrunk with increasing capture efficiency σ.

Further, increasing flux coverage α and/or surface coverage β can decrease the critical surface capillary length ξ_c and shift the critical wave number q_c toward short-wavelength regimes.

References

[1] M. Tssucgia, J.M. Gaines, R.H. Yar, R.J. Sines, P.O. Holtz, L.A. Coldrenand, P.M. Petroff, Phys. Rev. Lett. 62 (1989) 466.
[2] J.Y. Tsao, Materials Fundamentals of Molecular Beam Epitaxy, Academic Press, Boston, 1993.
[3] W.K. Burton, N. Cabrera, F.C. Frank, Philos. Trans. R. Soc. London: Ser. A 243 (1951) 299.
[4] A.A. Chernov, Modern Crystallography III, Springer–Verlag, Berlin, 1984, p. 15.
[5] G.S. Bales, A.Y. Zangwill, Phys. Rev. B 41 (1990) 5500.
[6] R.L. Schwoebel, J. Appl. Phys. 40 (1969) 614.
[7] G. Ehrlich, F.G. Hudda, J. Chem. Phys. 44 (1969) 1039.
[8] W.W. Mullins, R.F. Sekerka, J. Appl. Phys. 35 (1964) 1661.
[9] I. Bena, C. Misbah, A. Valance, Phys. Rev. B 47 (1993) 7408.
[10] Y. Kuramoto, T. Tsuzuki, Prog. Treor. Phys. 55 (1976) 356.
[11] I. Sivashiya, Acta Astraunautica 4 (1977) 1177.
[12] C. Misbah, W.-J. Rappel, Phys. Rev. B 48 (1993) 12193.
[13] F. Liu, H. Metiu, Phys. Rev. E 49 (1994) 2601.
[14] Y. Saito, M. Uwaha, Phys. Rev. B 49 (1994) 10667.
[15] A. Pimpinnelli, I. Elkinalni, A. Karma, C. Misbah, J. Villaain, J. Phys, Condens. Matter. 6 (1994) 1661.
[16] B. Houchmandzadeh, C. Misbah, Phys. Rev. Lett. 73 (1994) 94.
[17] M. Sato, M. Uwaha, Phys. Rev. B 51 (1995) 11172.
[18] M. Uwaha, Y. Saito, M. Sato, J. Cryst. Growth 146 (1995) 164.
[19] C. Misbah, O. Pierre-Louis, A. Pimpinelli, Phys. Rev. B 51 (1995) 17283.
[20] C. Misbah, O. Pierre-Louis, Phys. Rev. E 53 (1996) R4318.
[21] O. Pierre-Louis, C. Misbah, Phys. Rev. Lett. 76 (1996) 4761.
[22] C. Roland, G.H. Gilmer, Phys. Rev. B 54 (1996) 2931.
[23] M. Sato, M. Uwaha, J. Phys. Soc. Jpn. 65 (1996) 1515.
[24] M. Sato, M. Uwaha, J. Phys. Soc. Jpn. 65 (1996) 2146.
[25] Y. Saito, M. Uwaha, J. Phys. Soc. Jpn. 65 (1996) 3576.
[26] M. Sato, M. Uwaha, J. Phys. Soc. Jpn. 66 (1997) 1054.
[27] O. Pierre-Louis, C. Misbah, Y. Saito, J. Krug, P. Politi, Phys. Rev. Lett. 80 (1998) 4221.
[28] M. Sato, M. Uwaha, Y. Saito, Phys. Rev. Lett. 80 (1998) 4233.
[29] A.K. Myers-Beaghton, D.D. Vvedensky, Phys. Rev. B 42 (1990) 5544.
[30] A.K. Myers-Beaghton, D.D. Vvedensky, Phys. Rev. B 42 (1990) 9720.
[31] A.K. Myers-Beaghton, D.D. Vvedensky, Surf. Sci. 240 (1990) L599.
[32] J.W. Matthews, Epitaxial Growth, Academic Press, New York, 1975, p. 401.
[33] B. Carnahan, H.A. Luther, J. Wilkes, Applied Numerial Methods, Wiley, New York, 1969, p. 361.